COR-1B Pre- and Post-Vibration Tests, September 2004

William Thompson
October 2, 2004

This is a report on the results of performance verification measurements made of the COR-1B instrument before and after vibration in September 2004. The pre-vibration measurements were made on September 17-20, and were reported on in the COR-1B final assembly report. The post-vibration measurements were made on September 30 and October 1. Both sets of measurements were made in the COR-1 clean room facility in Building 5.

1 Focus

To measure the instrument resolution, an Air Force 1951 resolution test target was placed at the eyepiece location of a Meade telescope. To take the difference between nitrogen and vacuum focus into account, the target was moved back by a measured distance from the Meade's infinity focus.

Measurements were made at the following six locations on the detector, relative to the center of the CCD:

Location	X (mm)	Y (mm)
A	0	7
B	0	12.5
C	-5	-5
D	5	-5
E	-9	-9
F	9	-9

At each of the above points, measurements were made at 3 focus positions on the Meade telescope, centered around the nominal position of 8.7 mm, and at ± 1.5 mm. Figure 1 shows the results. The pre- and post-vibration results are essentially the same, within the measurement noise, and the uncertainty in the positioning.

2 Polarizer wedge

Measurements of the Air Force resolution target, made every 15°, can be used to derive the amount of image motion as a function of polarizer position. The post-vibration measurements show that the target image makes a small circular motion with a radius of 0.26 pixels (3.5 μm, 0.97 arcsec), and a phase angle of -34.°0. Although the magnitude of the motion agrees well with the pre-vibration measurements, the phase and direction of the motion is quite different, which is evidence that a small change in the polarizer wedge occurred. The pre- and post-vibration measurements are shown in Figure 2.

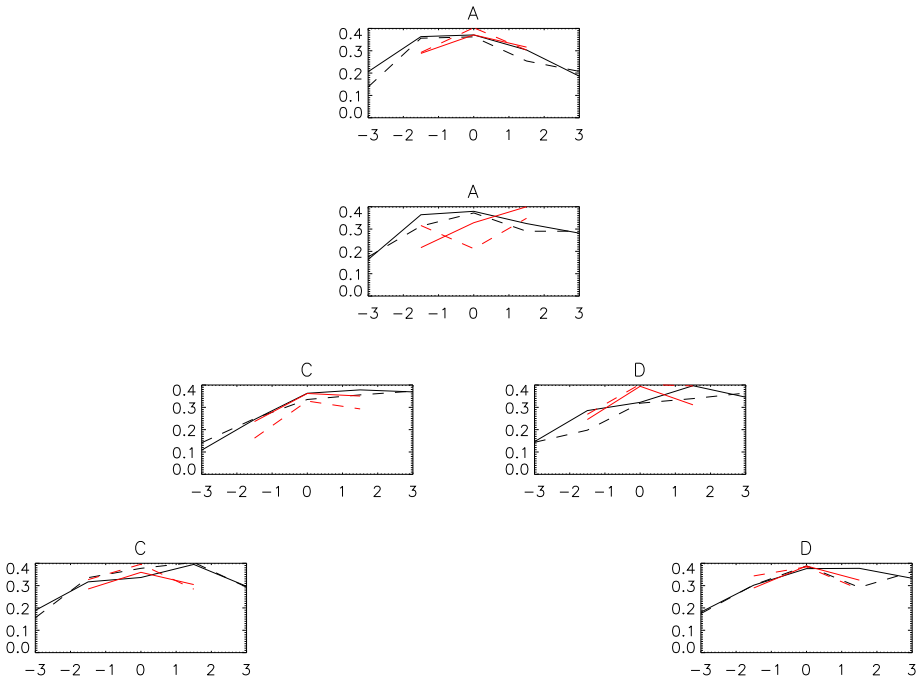

Figure 1: Contrast values as a function of Meade focus for several positions on the detector. Solid lines are for vertical bars, dashed for horizontal bars, black for pre-vibration, red for post-vibration.

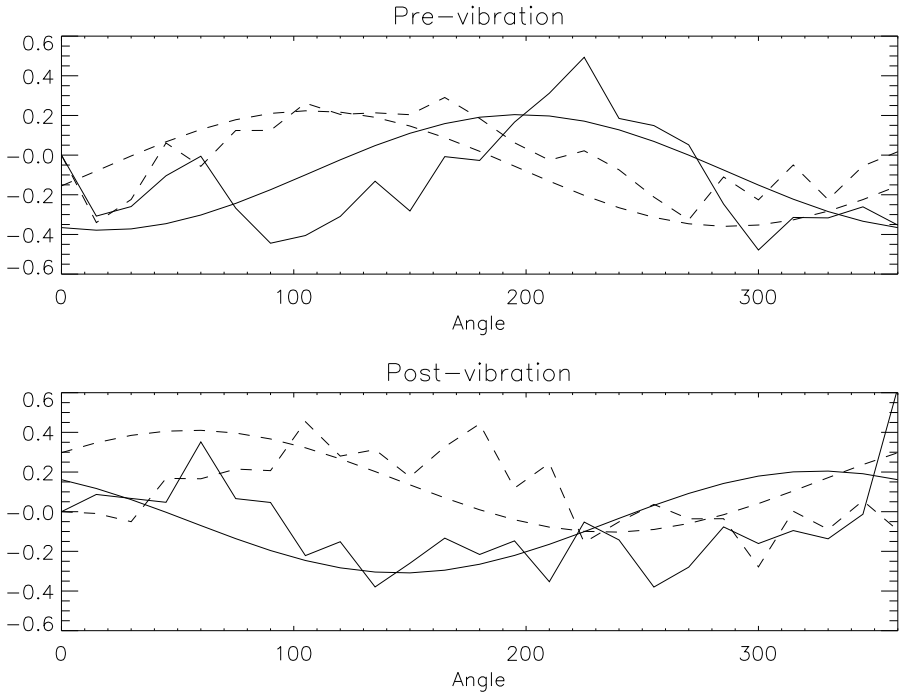

Figure 2: Target position as a function of polarizer angle, relative to the position at 0°, in the X (solid) and Y (dashed) directions. Also shown are the curves representing the fitted circle.

There is a possibility that the wedge results are affected by the detector readout electronics. It has been noted that sometimes the image shifts left-to-right on the detector by one pixel, presumably because of communication errors along the extra-long spacewire cable between the CEB and the Linux PC. In Figure 2 it can be seen that the y-axis behavior is the same pre- and post-vibration, and that the difference is in the x-axis behavior. If part of the x-axis data is affected by spacewire communication errors in either the pre- or post-vibration data sets, that could explain the discrepency.

The spacewire cable used in the vacuum calibration tests at NRL is shorter, and shouldn't be subject to the same problems.

3 Focal plane mask

Illuminating the front aperture with the NRL "Sun bucket" allows one to test the alignment between the occulter and the focal plane mask. If either shifts relative to the other, then the sharp diffraction features from the occulter edge would appear in the image. Measurements made before and after vibration show that this did not occur, as demonstrated in Figure 3. The light levels in the pre-vibration measurements are comparable to those seen for COR-1A. However, the light levels in the post-vibration measurements are much higher. This is because the thermal shield was in place, reflecting light back onto the source, which then scatters it back again into the image. This was the first time that the "Sun bucket" test was performed with the thermal shield in place. Similar effects from the thermal shield were seen during the vacuum testing of COR-1A.

4 Exposure time test

The procedure EXPTIMETEST takes a series of exposures ranging from 0.1 to 10 seconds, together with the associated dark images. Intercomparing the resulting images allows the accuracy of the exposure times to be explored. To keep the instrument from saturating at the longer exposure times, the lamp current was reduced from 6 to 4 amps. Even so, some saturation occured at the longest exposure times due to dark current in the room temperature CCD.

Two keywords in the FITS headers are related to the exposure times. The keyword EXPCMD contains the commanded exposure time, while EXPTIME contains the measured exposure time, based on the motion of the shutter mechanism. For dark images, EXPTIME is calculated using a different algorithm, and is not reliable. Figure 4 shows the difference between the measured and commanded exposure times. The post-vibration results are essentially identical to the pre-vibration measurements.

Figure 5 demonstrates that the relationship between the exposure time and the measured signal in the detector is linear. The behavior is the same as the pre-vibration measurements, and differs only in that the lamp brightness was not the same between the two tests.

Figure 3: Focal plane mask measurements before and after vibration. The scattered light in the post-vibration image is higher, because the thermal shield was in place.

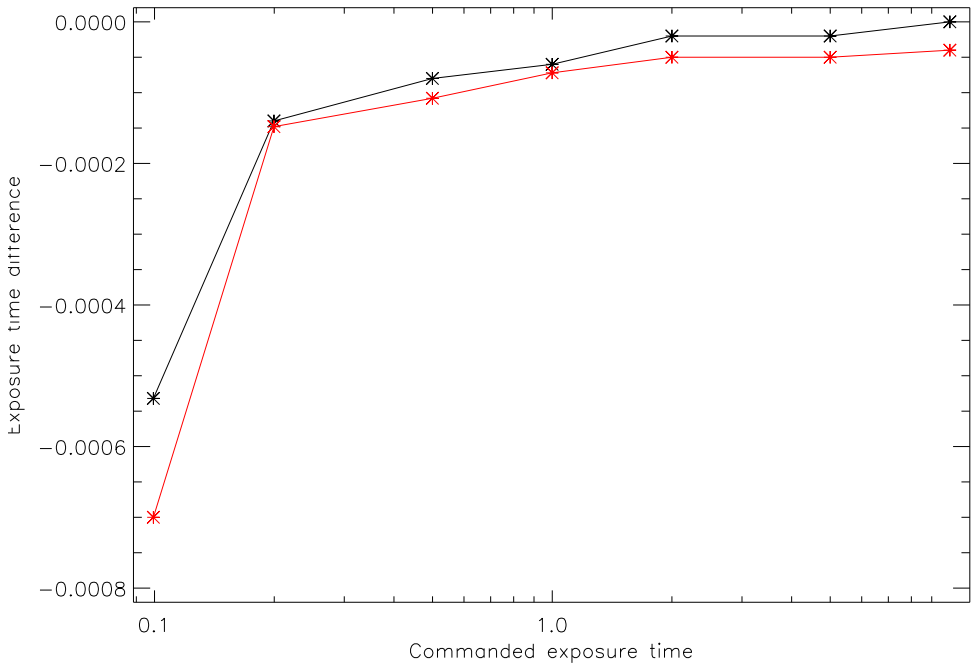

Figure 4: Difference between measured and commanded exposure times. Black: pre-vibration, red: post-vibration.

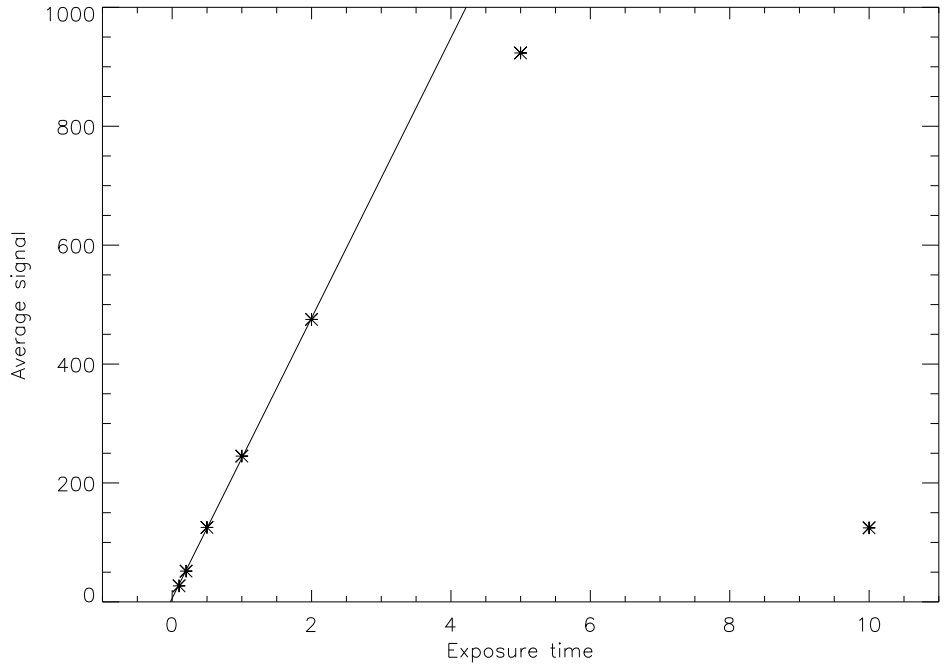

Figure 5: Comparison between measured signal and exposure time. The longer exposure times are affected by saturation in the detector.

5 Light leak testing

To see if there were any light leaks in the instrument, a series of exposures were taken with a bright flashlight shone on the interface between each tube section, on the FPA mount plate, and on each Mott filter. No light leaks were seen.

6 Boresight

To be added.

7 Flat field test

When analyzing the flat field data from COR-1A, an attempt was made to detect subtle motions of the occulter and focal plane mask by looking at the detailed shape of the penumbral shadow, as expressed by the equation

$$r = a_0 + a_1 I + a_2 I^2 \tag{1}$$

where r is the pixel position, and I is the rescaled brightness. However, it appears that many of the subtle changes in the flat field were actually due to the illumination pattern on the front window. This is demonstrated in Figure 6, which compares the shape of the penumbral shadow for three cases where the lamp in front of the window was moved between tests. The inner and outer edges of the penumbra are relatively insensitive to lamp placement, while the a_1 and a_2 parameters change with lamp placement. Figure 7 demonstrates that the position of the penumbral edges did not change after vibration.

8 Conclusions

No changes were seen in the instrument focus or alignment after vibration. A small change was seen in the polarizer wedge, but this may simply be due to the readout electronics.

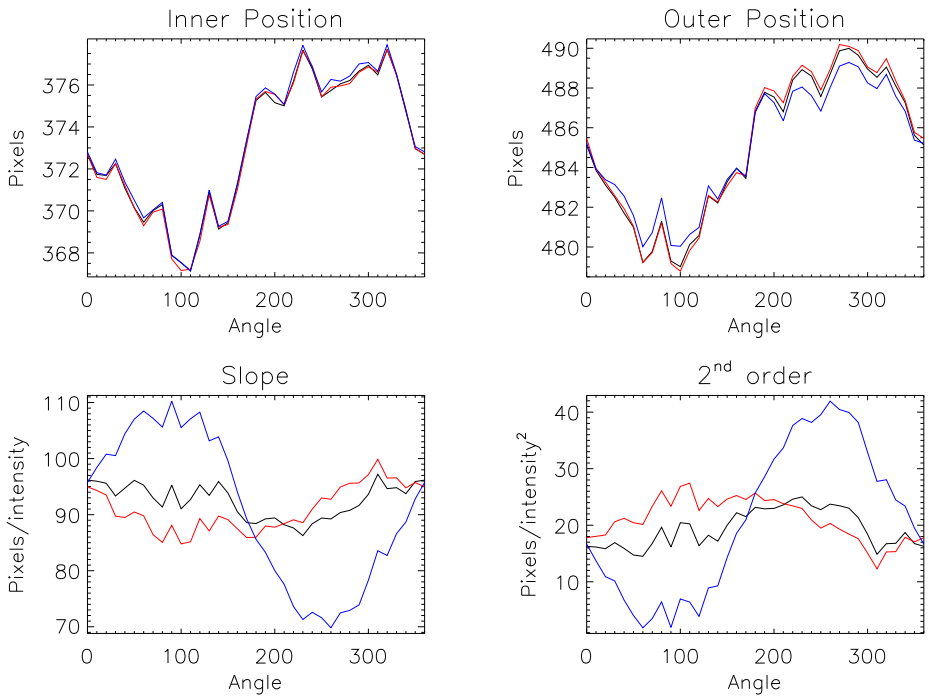

Figure 6: Results of fitting Eq. 1 to three flat field images, where the only difference between the images was the placement of the lamp in front of the instrument door. The top two plots show the extrapolations of the curves to $y = 0$ and $y = 1$, which represent the inner and outer edges of the penumbra. The bottom two plots show the parameters a_1 and a_2 respectively.

Figure 7: Plots of the inner and outer edges of the penumbra as a function of angle. Black: pre-vibration, red: pos-vibration.